Dependence of the emission from tris(8-hydroxyquinoline) aluminum based microcavity on device thickness and the emission layer position

A. B. Djurišić,[*] C. H. Cheung,[*] C. Y. Kwong,[†] J. Chan,[&] A. D. Rakić,[&] H. L. Tam,[‡] K. W. Cheah,[‡] Z. T. Liu,[*] W. K. Chan,[◊] and P. C. Chui,[†]

[*]Dept. of Physics, University of Hong Kong, Pokfulam Road, Hong Kong

[†] Dept. of Electrical & Electronic Engineering, University of Hong Kong, Pokfulam Road, Hong Kong

[&] School of Information Technology and Electrical Engineering, The University of Queensland, Brisbane Qld4072, Australia

[‡] Dept. of Physics, Hong Kong Baptist University, Kowloon Tong, Hong Kong

[◊] Dept. of Chemistry, University of Hong Kong, Pokfulam Road, Hong Kong

In this work, we present a systematic study of the emission from bilayer organic microcavity light emitting diodes with two metal mirrors. The devices consisting of two organic layers, N,N′-di(naphthalene-1-yl)-N,N′-diphenylbenzidine (NPB) as a hole transport layer and tris (8-hydroxyquinoline) (Alq) as emitting layer, and two metal mirrors were fabricated and characterized by transmission, reflectance, photoluminescence, and electroluminescence measurements. The effects of layer thickness, interface position, and the choice of anode (bottom mirror) were investigated. The transmission and reflectance spectra were modeled using a transfer matrix model, and the optical functions for all the materials used were determined by spectroscopic ellipsometry. The calculated and experimental data are in good agreement. The

dependence of the photoluminescence and electroluminescence spectra on the device thickness and interface position is discussed.

PACS: 85.60.Jb; 85.60.Bt

1. INTRODUCTION

Organic materials have been attracting lots of attention for application in organic light emitting diodes (OLEDs) due to their potential high brightness and possible inexpensive fabrication on large area and/or flexible substrates. A large number of different materials for OLED application have been developed in recent years. In addition to the research on novel materials, novel device structures have been investigated as well. Among those, microcavity OLEDs have been attracting lots of attention in order to achieve spectral narrowing, brightness enhancement, or multipeak emission from the same emitting layer.[1-5] In addition to interest for practical applications, microcavity structures are also of interest for fundamental physics studies. In particular, strong coupling phenomena in organic microcavities are of interest due to large values of Rabi splitting which can be observed at room temperature.[6-14] It is commonly accepted that, in order to achieve strong coupling in an organic microcavity, the organic material should have narrow absorption spectrum.[11] Therefore, majority of the studies of strong coupling have been confined to the systems of limited importance for practical applications, such as cavities containing porphyrin or cyanine dyes doped into a polystyrene or polyvinyl alcohol matrix.[7,9-14] However, very large Rabi splitting was reported for the polysilane based microcavities,[6] in spite of the fact that the linewidth of polysilane (~190 meV)[6,8] is about twice as large as that of more commonly used organic materials in cavities exhibiting strong coupling.[11,13]

It should be noted, however, that narrow linewidth is not a mandatory requirement to achieve strong coupling. The necessary condition for the strong coupling to occur in a

microcavity is that the emitted photon is reabsorbed before leaving the cavity and it can be expressed as[15]

$$\alpha_e d >> \pi / F \,, \tag{1}$$

where α_e is the absorption coefficient, d is the length of the absorbing medium, and F is the cavity finesse. The condition for the observation of the strong coupling can be also stated as:[16]

$$\Omega_0 > \delta_c + \gamma \,, \tag{2}$$

where Ω_0 is the on-resonance splitting (which is not necessarily the same for reflectance, transmission, absorption, and photoluminescnce[17]), γ is the homogeneous oscillator linewidth, and δ_c is the linewidth of the cavity mode. Neither of these two conditions is very stringent. Organic materials typically exhibit relatively large absorption coefficients so that for a sufficiently large layer thickness the condition given by Eq. (1) can be easily satisfied even in microcavities which do not have a large finesse. It was demonstrated that a low Q factor cavity with two metal mirrors resulted in larger Rabi-splitting than a cavity with one metal and one highly reflective Bragg mirror.[7] Considering the reported large values of Rabi splitting in the organic materials, which can be as high as 0.43 eV,[6] it is clear that the condition expressed by Eq. (2) can also be easily satisfied, even for material with linewidths larger than those commonly used to investigate strong coupling phenomena. However, the presence of peak splitting is not a sufficient indication of strong coupling.[16] It is possible to observe more than one photoluminescence peak, without anticrossing of the exciton and photon modes which indicates the strong coupling.[16] Furthermore, the splitting between TE and TM modes can occasionally cause peak splitting which is rather similar to the Rabi splitting.[18] Although previous works on

the angular dependence of the emission from the Alq based microcavities showed blue shift but no peak splitting,[1-3] based on the differences in the angular dependence of the phase change upon reflection from the silver mirror for two polarizations,[5] observation of TE and TM mode splitting would not be unexpected.

In this work, we fabricated and characterized organic microcavity structures with two metal mirrors and N,N′-di(naphthalene-1-yl)-N,N′-diphenylbenzidine (NPB) as a hole transport layer and tris (8-hydroxyquinoline) (Alq) as emitting layer. Silver (70 nm) was used as a cathode and top mirror, while either thin (25 nm) Cu or thick (80 nm) Ag where considered as a bottom mirror. The fabricated devices were characterized by transmission (T), reflectance (R), photoluminescence (PL), and electroluminescence (EL) measurements. The transmission and reflectance were also modeled using a transfer matrix model, and the index of refraction of all the materials used was determined by spectroscopic ellipsometry. The properties of the devices as a function of total device thickness, bottom mirror, and the position of the NPB/Alq interface were studied. In the case of a thick Ag mirror, very clear peak splitting is observed for larger viewing angles. The calculations indicated that the observed peak doublet was due to TE and TM mode splitting, which was also confirmed by PL measurements with a polarizer. However, in the devices with thin Cu mirror, unusual behavior involving multiple peaks in electroluminescence whose intensity ratio changes with the viewing angle is observed. Possible reasons for this behavior are discussed.

The paper is organized as follows. In the following section, details on the device fabrication and characterization are given and the model for calculations of the spectra is

described. In section III, obtained results are presented and discussed. Finally, conclusions are drawn.

2. EXPERIMENTAL AND CALCULATION DETAILS

In this section, we will describe sample preparation, determination of the index of refraction of materials using spectroscopic ellipsometry, device characterization using R, T, PL, and EL measurements, and finally calculation of the R, T, and emission spectra.

A. Sample preparation

The NPB and Alq (from H. W. Sands) were purified by sublimation before device fabrication. Both devices and thin films for spectroscopic ellipsometry measurement were fabricated by evaporation in high vacuum (~10^{-6} Torr). The layer thickness during deposition was displayed by a quartz thickness monitor, and it was double checked after deposition using step-profiler and ellipsometry. Thin films for the spectroscopic ellipsometry measurements were fabricated either on Si or glass substrates. For Alq and NPB, films on silicon substrates were used in order to obtain better signal since the reflectivity of NPB or Alq on a glass substrate is low. It was reported that the extinction coefficient values for thin films with low refractive index on a transparent substrate follow the sign and magnitude of the spectral noise.[19] In addition, it was reported that the overestimation of the extinction coefficient of transparent glasses cannot be eliminated by surface roughness correction.[20] In our previous study of thin Alq films on a glass substrate, possible overestimation of the extinction coefficient in sub-band gap range was obtained.[21] For these reasons, Si substrate was used for the organic layers. Since it was shown that the Alq deposited on unheated substrate is amorphous,[22] no significant influence of the substrate on the film structure and optical properties is expected. For

copper and silver, films on glass substrates were fabricated. The back surface of the glass substrate was made rough in order to eliminate errors due to reflections from this surface. All the substrates were cleaned by acetone, ethanol, and DI water.

MOLED devices had following structure: quartz/bottom mirror/NPB/Alq/Ag (70 nm). The devices with different bottom mirror (Cu and Ag) were fabricated at the same time in order to eliminate possible effects of the thickness variation of the organic layers. In addition to MOLEDs containing NPB and Alq layers, MOLEDs with Alq layer only with the same total thickness were also fabricated in order to exclude possible effects of NPB on the observed phenomena. The MOLEDs with NPB/Alq and Alq layers exhibited similar behavior, except that the blue emission from NPB upon 325 nm excitation was absent in MOLEDs containing only Alq.

B. Material characterization

Thin films of Alq, NPB, silver, and copper were measured by an ellipsometer (J. A. Woollam V-VASE variable angle spectroscopic ellipsometer). Photoluminescence (excited at 325 nm by a HeCd laser) and absorption (using Hewlett Packard 8453 UV-Vis spectrometer) measurements for the NPB and Alq films were also performed. Ellipsometric measurements were taken at the incident angles of 65, 70, and 75 degrees, in the wavelength range of 300 – 1000 nm. For each sample, several measurements were taken at different sample orientations to verify the in-plane isotropy of the films. Then the experimental data were fitted to obtain the refractive indices of the materials, which were described by a Lorentz model for Alq and NPB, and by a Lorentz-Drude model for silver and copper. Simulated annealing algorithm was used as the optimization method, similar

to our previous study.[21] The complex dielectric function according to the Lorentz oscillator model[21] is described as:

$$\varepsilon = \varepsilon_{\inf} + \sum_m \frac{F_m}{\omega_m^2 - \omega^2 + i\Gamma_m \omega} \quad , \tag{3}$$

where ε_{inf} is a constant, m is the number of oscillators with a frequency ω_m, broadening constant Γ_m, and oscillator strength F_m. For modeling the dielectric function of Cu and Ag, the Lorentz-Drude[23] model was used

$$\varepsilon = \varepsilon_{\inf} - \frac{F_0}{\omega^2 - i\Gamma_0 \omega} + \sum_m \frac{F_m}{\omega_m^2 - \omega^2 + i\Gamma_m \omega} \quad , \tag{4}$$

where F_0 and Γ_0 are the oscillator strength and the broadening constant, respectively, for the intraband transitions.

C. Device characterization

HeCd laser (325 nm), Xe lamp (420 nm), and Ar ion laser (488 nm) were used as the excitation sources for photoluminescence (PL). The excited spectra were collected using a double monochromator (1.4 m Oriel 77225) with Peltier-cooled photomultiplier detector (Hamamatsu R636-10). For the electroluminescence (EL) measurement, a Keithley 2400 sourcemeter was used to bias the devices, and the EL spectra were recorded using a fiberoptic spectrometer PDA-512-USB (Control Development Inc.). A deuterium-tungsten lamp and a 1000 W Xenon lamp were used as excitation sources for reflectance and transmittance measurements, respectively (higher power Xe lamp was required for T measurements due to weak signal for MOLEDs with thick Ag mirrors), and the spectra were collected in the same manner as for the PL. For time resolved photoluminescence measurements, a HP 54522A oscilloscope was used to capture the

decay curve following an excitation pulse from a Nd:YAG laser (355 nm third harmonic line).

D. Device modeling

The reflectance and transmittance of the devices were modeled using a transfer matrix model.[24-26] The calculated results were corrected for the incoherent reflection from the backside of a quartz substrate.[27-29] The refractive indices for all the thin film layers in the structure were determined by spectroscopic ellipsometry. For the quartz substrate, the refractive index was described by a Cauchy equation fit of the data tabulated in Ref.[30]

The emission spectra were modeled using the following equation:[4,31-33]

$$I_{cav}(\lambda) = \frac{\frac{1-R_{bot}}{i}\sum_{i}\left[1+R_{top}+2\sqrt{R_{top}}\cos\left(\frac{4\pi z_i}{\lambda}-\varphi_{top}\right)\right]}{1+R_{bot}R_{top}-2\sqrt{R_{bot}R_{top}}\cos\left(\frac{4\pi L}{\lambda}-\varphi_{top}-\varphi_{bot}\right)} I_{nc}(\lambda), \quad (5)$$

where $L=\sum_j n_j d_j$ is the optical thickness of the cavity, z_i is the optical distance of the emitting dipoles to the metal mirrors, $I_{nc}(\lambda)$ is the free space emission of Alq (determined from the photoluminescence measurements of the Alq film), and the summation over i is performed assuming that the dipoles are located within 20 nm from the HTL/Alq_3 interface.[32] The summation is performed with 1 nm step. In all calculations, the signs for phase angles were taken to be consistent with the exp($j\omega t$) convention, and hence the complex index of refraction of the materials was described by $N=n-ik$.[31]

3. RESULTS AND DISCUSSION

The fabricated thin films were first characterized by spectroscopic ellipsometry. The determined refractive indices were then used to model the MOLED devices.

MOLEDs with different bottom mirrors and different thickness of the organic layers were fabricated and characterized by R, T, PL, and EL measurements.

A. Optical properties of materials

Figures 1 and 2 show the experimental and calculated TanΨ and CosΔ values for the Alq and NPB films on Si substrates, respectively. Very good agreement between the calculated and the experimental data can be observed for all three incident angles. Three oscillators were used to model the index of refraction of Alq, while two oscillators were sufficient for NPB. The obtained parameters are listed in Table I, and the real and imaginary parts of the refractive index are shown in Fig. 3. Unlike our previous work,[21] conventional Lorentz oscillator model was sufficient to obtain good agreement with the experimental data. This is possibly due to more narrow spectral range considered. Some reduction in the inhomogeneous broadening component due to different source and improved purity of the material is also possible. Better quality of the experimental data because of higher sample reflectance and smoother sample surface due to Si substrate may also play a role. The obtained refractive index value of the Alq is somewhat lower than that in the other works reported in the literature.[34-37] Differences in the obtained optical properties are most likely due to the differences in the purity of the source material, vacuum level during the deposition, as well as the deposition rate. Since we fabricate MOLEDs in the same evaporation system and under the same condition as the films for ellipsometry, the optical functions determined by our measurements are more appropriate for the modeling of our MOLED devices. For NPB, there are no refractive index data available, so that no comparisons with the literature can be made.

Figures 4 and 5 show the calculated and experimental TanΨ and CosΔ values for Cu and Ag thin films for three different incident angles. The data were fitted using Lorentz-Drude model, with one oscillator for silver and three oscillators for copper. Lorentz-Drude model for these two materials is satisfactory for the spectral range considered. If wider spectral range is needed, the use of other more complex models may need to be considered.[23] Very good agreement between the experimental and calculated values can be observed. The obtained model parameters are given in Table I, while Fig. 6 shows the obtained real and imaginary parts of the index of refraction. The reference data for Ag and Cu from the ellipsometry software are also shown for comparison. While same trends can be observed in our and the reference data, there are some differences which are more pronounced for Cu films. This is not unexpected, since there is large scatter of the reported values in the literature for all metals.[38] One of significant contributing factors to the differences in the optical properties are different methods of sample preparation.[38] It was shown that, for example, the reflectance of the evaporated aluminum films depends on the vacuum level and the evaporation rate.[39] Due to differences in the sample preparation, it is highly advisable to experimentally determine the optical functions of thin films used for the device fabrication rather than use the available data in the literature.

B. Microcavity devices results and discussion

In the following, different devices will be labeled according to NPB and Alq thickness, for example 65/139 for the device with 65 nm NPB and 139 nm Alq. Also, where necessary, spectra for different viewing angles will be vertically shifted for clarity. All the emission spectra are normalized for easier comparison of the peak positions.

Figures 7 and 8 show the electroluminescence and photoluminescence spectra of the 65/139 device for different viewing angles. Electroluminescence was measured through the semitransparent Cu mirror, while PL could be measured through both top and bottom mirror. Significant difference between EL and PL (both measured from the substrate side, Fig. 7 and Fig. 8a) can be observed. The photoluminescence spectra consist of two peaks, a higher intensity blue green exhibiting blue shift with increasing viewing angle and a lower intensity yellow-green peak which does not show significant shift with increasing viewing angle. The position of this peak is red-shifted compared to the free space emission from Alq. On the other hand, EL spectra show two peaks of almost equal intensity. Neither of the peaks exhibits significant shift with the increasing viewing angle, but their intensity changes. The emission spectra from the side of the substrate show typical green Alq emission. Therefore, the observed unusual features are definitely a result of the interplay of the cavity and the emitting material. The differences between EL and PL spectra can originate from NPB emission contribution in the PL, different position and width of the emissive layer, as well as possible effects of the applied electric field. Some differences due to different emission region position can be inferred from the differences in the PL spectra measured through the bottom and top mirror (Fig. 8a and b), although the behavior of both PL spectra with changing viewing angle is fundamentally different from the EL spectra.

In order to further investigate this phenomenon, we have fabricated the devices with ½ and two times the thickness of the original one. The PL spectra for 33/69 and 130/278 devices with thin Cu mirrors are shown in Fig. 9. The 130/278 was too thick to show any electroluminescence, while the EL spectra of the 33/69 device were very

similar to the PL spectra. The PL spectra from the top electrode of 33/69 device show some NPB emission, but otherwise exhibit similar behavior with viewing angle. Similar behavior between EL and PL spectra is also observed in the 33/69 devices with Ag bottom mirror, as shown in Fig. 10. For both EL and PL, blue shift of the emission with clear TE and TM mode splitting at higher viewing angles can be clearly observed, as expected. On the other hand, 130/278 device exhibits more complex behavior due to appearance of additional cavity modes. When we compare the spectra from 33/69, 65/139, and 130/278 devices, we can see that in spite of obvious differences there are some common features. For example, 65/139 and 130/278 devices have one resonance at 470-480 nm, some weaker emission in the region 530-580 nm, while additional mode at ~630 nm is absent in 65/139 due to shorter cavity length. The shoulder due to NPB emission can be observed for both 33/69 and 130/278 devices. The most significant difference, however, is very broad emission from 33/69 device with Cu mirror. The position and the width of this emission are different from that obtained for 65/139 and 130/278 devices, but its position agrees well with the lower energy EL peak in the 65/139 device. 33/69 device with two Ag mirrors does not exhibit increased linewidth of the emission. Also, 33/69 appears to be the only device where the differences between the PL spectra from the top and bottom mirror are small, as well as the differences between the EL and PL spectra. However, it should be noted that the positions of the peaks in PL spectra from the top and bottom mirror in 65/139 and 130/278 devices are similar, but their relative intensities are different. This is possibly due to excitations of different regions due to different optical properties of NPB and Alq, as well as different transmission of the top and bottom mirrors.

In order to investigate further observed unusual phenomena in the devices with thin Cu bottom mirror, we fabricated devices with the same total thickness, but different position of the NPB/Alq interface. The obtained EL and PL spectra for 153/51, 102/102, 51/153, and 26/178 devices are shown in Fig. 11 and Fig. 12. It is obvious that the interface position and the Alq thickness play a significant role in the obtained results. It can be observed that the emission from the near-infrared cavity mode (700-800 nm) becomes visible only for the devices with large Alq thickness. It is well known that the Alq exhibits subband gap absorption[40,41] Still, it is surprising that the emission above 700 nm can be excited in Alq based microcavities. It should be noted that previous studies found that the emission in Alq consists of three different transitions, but the proposed energies of these transitions were different.[42,43] Cury and Gillin[42] proposed that the lowest energy (2.04 eV) transition originated from triplet recombination, which is in agreement with the theoretically predicted energy level of a triplet state (~2.14 eV).[44] However, time resolved photoluminescence study by Humbs *et al*.[43] yielded no evidence of triplet emission and resulted in different energy levels for the three transitions. We have also performed time resolved photoluminescence measurements for our microcavity devices, and in all cases (green as well as near-infrared emission) obtained decay times were in the range of 10-20 ns, similar to the value obtained for Alq films. For the Alq films, we obtained decay times in the range 16-18 ns, which is in good agreement with the results reported in the literature.[45-48] Based on the time resolved photoluminescence results, involvement of triplet states in the observed emission does not seem likely. However, the fact that the lower energy emission appears only in devices with large Alq thickness

indicates that sub-band gap states with low absorption and luminescence intensity may play an important role in the observed behavior.

In order to exclude the possible influence of the NPB layer, we fabricated the microcavity devices containing only Alq with the same total thickness (204 nm). Obtained photoluminescence results for microcavities with bottom Cu and Ag mirrors are shown in Fig. 13. For the microcavity device with Cu mirror, a broad feature which likely consists of two peaks and which does not show significant blue shift with the viewing angle can be observed. For larger viewing angles, the peak corresponding to near-infrared cavity mode which shows blue shift with increasing viewing angle becomes visible. Therefore, this emission indeed originates in the Alq and it is not a result of formation of a complex at the Alq/NPB interface. For a thick Ag mirror, we can observe more complex behavior, as shown in Fig. 13b. For small viewing angles, narrow blue peak can be observed. With increasing viewing angle, broad green emission increases and becomes pronounced at ~50° viewing angle. With further increase of viewing angle, both blue and green emission intensities reduce, and the intensities of the two near-infrared peaks (peak splitting due to TE and TM modes) increase. As it can be clearly observed, the observed spectra show complex behavior even in the absence of an NPB layer. More importantly, the obtained results appear to be strongly dependent on the bottom mirror reflectance. The influence of the bottom mirror (thin Cu vs. thick Ag layer) is also illustrated in Fig. 14, showing the PL from the top mirror side for 153/51 and 51/153 devices with Cu and Ag bottom mirrors. In both cases it can be clearly observed that the behavior of the devices with bottom Ag mirror is rather similar. A green narrow peak exhibiting blue shift and polarization mode splitting with increasing viewing angles can be observed. The

peak position exhibits some dependence on the Alq layer thickness and the interface position, but overall behavior is the same. This is not the case for the devices with thick Cu mirror, where notably different behavior with increasing viewing angle can be observed for different devices.

In order to identify the factors affecting the emission spectra, we have performed simulations of the emission from different devices. The comparison between the calculated and experimental spectra is shown in Fig. 15. It can be observed that the main features of the spectra agree reasonably well, but that there are differences between the calculated and experimental spectra. One possible reason is discrepancy between the actual and assumed thickness, which cannot be entirely excluded in spite of the careful calibration of the quartz thickness monitor based on the post-deposition measurements of thickness using both ellipsometry and step-profiler. Another possible reason is different width of the emission region. The effects of varying the width of the emission region are shown in Fig. 16. It can be observed that, while the emission region width does not affect the spectra significantly in the case of the 80 nm Ag mirror, significant differences among the spectra corresponding to different emission region width can be observed for thin Cu mirror. Therefore, one possible explanation for differences between calculated and measured spectra could be the emission region width, which was assumed to be equal 20 nm in all cases. The difference in the emission region width could also at least partly account for the differences between the EL and PL spectra. It should also be noted that the differences in the simulated spectra for different assumed emission region width become more pronounced for larger Alq layer thickness. The position of the NPB/Alq interface affects the nature of the influence of emission region width. For the devices of

½ /½ type (i.e. 50/50, 100/100 etc.), for large thickness increase of the emission region width results in the blue shift of the emission. For devices of the type ¼/¾ (i.e. 25/75, 50/150, etc.), different emission region width results in different intensity ratios of the two peaks. One possible explanation for different emission region width may be due to large difference in the electron and hole mobilities in Alq and NPB, respectively.[50] Hole mobility in the NPB is about two order of magnitude larger than the electron mobility in Alq.[50] It is well known that there are charges at the Alq/NPB interface in an OLED.[51-54] Fixed negative charges were found at NPB/Alq interface,[51,52] as well as the accumulation of the positive charges during the device operation.[53,54] The negative interfacial charge density was found not to be dependent on the Alq thickness based on the linear dependence of the transition voltage on Alq thickness.[51,52] On the other hand, additional positive charge can be found in the bulk of the Alq layer and the amount of this charge increases with the device aging and the dependence of the transition voltage on Alq thickness is no longer linear.[54] Since the emission region width is determined by the exciton diffusion length,[55] it is possible that it can be affected by different electric field distribution in the devices with different Alq thickness. It should also be noted that the change of the emission region width decreases with increased operation time,[56] which may be related to the accumulation of the positive charges.[54] The emission region width was also found to be dependent on the voltage for low bias voltages,[57] although this phenomena are not likely to play a significant role in the results presented in this work since no significant dependence of the spectra on bias voltage was noted. This is likely because the low bias voltages resulting in low luminance could not be coupled via fiber into the spectrometer.

We also performed photoluminescence measurements for different excitation wavelengths, as shown in Figs. 17 and 18. Figure 17 shows the PL spectra of 33/69, 65/139, and 130/278 devices excited at 420 nm. It can be observed that for 130/278 the spectra excited at 325 nm (Fig. 9b) and 420 nm (Fig. 17c) are rather similar. The main difference is the absence of NPB emission (a shoulder observed at low viewing angles in Fig. 9b). For 33/69 device, some differences for different excitation wavelengths (Fig. 9a and Fig. 17a) can be observed. When the device is excited with 420 nm, two peaks can be resolved in the broad emission in the 500-700 nm range. For 65/139 device, green instead of blue green emission is observed at 420 nm excitation. The difference can be partly due to the absence of NPB emission, although enhancement of the yellow emission contribution at 420 nm excitation is not fully clear. If we compare the PL spectra of the microcavities containing only Alq layer excited at different wavelengths (325 nm excitation shown in Fig. 13a, 420 nm and 488 nm excitations shown in Fig. 18 a and b, respectively), it can be observed that the excitation wavelength significantly affects the PL spectra. At 325 nm, a broad feature likely consisting of two peaks can be observed, and additional near-infrared peak is seen at higher viewing angles. No near-infrared emission is seen at 420 nm and 488 nm excitation, and for both excitation wavelengths emission is dominated by a single peak, green with weak yellow emission for 420 nm excitation and yellow for 488 nm excitation. No differences in the emission spectra from an Alq film were observed when the excitation wavelength was changed. It should be noted that it is unexpected that excitation at 488 nm results in any PL, which indicates significant contribution of the sub-gap states in the Alq emission.

All the fabricated microcavity devices were also characterized by reflectance and transmittance measurements. The devices with the same bottom mirror exhibit very similar behavior. The obtained results (calculated and experimental) for 51/153 device are shown in Fig. 19. Good agreement between the main features of the experimental and calculated spectra can be observed. There is some difference in the transmittance intensity, which is likely due to different factors for coupling into the fiber at different incident angles. The spectra from devices with Cu mirror show broad minimum whose shape changes with increasing viewing angle. The comparison of the measured reflectance spectra for Alq only device for Cu and Ag bottom mirrors is shown in Fig. 20. It can be observed that the device with thick Ag mirror show two cavity modes. The longer wavelength mode also exhibits clear polarization mode splitting, similar to the transmittance and PL spectra.

From all the obtained results, it is clear that the devices with two thick Ag mirrors behave as expected based on other organic microcavity works in the literature.[1-3,5] One possible exception is 204 nm Alq only microcavity, where the reasons for change of dominant emission mode from blue to near-infrared with increasing viewing angle require further study. On the other hand, all devices with bottom Cu mirror exhibit some unusual behavior, which becomes more pronounced with increasing Alq thickness. We have plotted the peak positions as a function of the viewing angle for Alq only and 51/153 microcavities, as shown in Figs. 21 and 22, respectively. For thin Cu mirror, the transmission peak positions were fitted with three coupled oscillator model[12,13] for 204 Alq cavity, while for 51/153 microcavity two coupled oscillator model[8] was used. This is because three peaks can be observed in the former case, while there are two peaks in the

latter case. For the 204 nm Alq device with Ag mirror, two branches observed in the PL, R, and T at about 2.65 eV and 1.4 eV (normal incidence) correspond to the two cavity photon modes. The additional emission peak at ~2.4 eV is possibly due to uncoupled emission from the Alq, although it is somewhat shifted compared to the position of the PL peak from the Alq film (at 2.27 eV). For 51/153 device, second mode lies further in the infrared (as can be seen from the R and T spectra at higher incidence angles, as shown in Fig. 19) so only one branch with polarization mode splitting can be observed. The devices with Cu mirrors show more complex behavior. Peak positions can be fitted with coupled oscillators model and the curves show anticrossing behavior. It should be noted that the presence of multiple peaks in the emission spectrum is not a proof of the polariton emission.[16] However, anticrossing of the curves can be considered as an indication of strong coupling.[16] The difference between the peak positions obtained from different measurements is more pronounced in devices with lower reflectivity (Cu) mirror, which is in agreement with the theoretical predictions.[17] Also, the separation of the branches for different measurements is higher for transmittance than for reflectance, which would be expected in a microcavity with larger detuning and lower bottom mirror reflectance.[17] The obtained results appear to indicate possible polariton emission in the microcavities with thick Alq layer and low reflectivity bottom mirror. Strong coupling in a low Q factor cavity with two metal mirrors was demonstrated for a different organic material.[7] Thus, polariton emission in our devices is not impossible although it is unexpected since Alq exhibits rather broad emission (although the cavity mode also has relatively large width due to low Cu mirror reflectivity). However, further experiments, such as time resolved photoluminescence following ultrafast excitation[10] are needed to

confirm whether the observed phenomena are indeed a consequence of the polariton emission. In addition, the nature of the tail states contributing to the observed near-infrared emission also requires further study.

Finally, in order to verify whether the observed unusual features are a consequence of the use of Cu mirror, we fabricated 204 nm Alq microcavities with Ag (17 nm), Au (28 nm), and Cu (60 nm) mirrors. PL spectra of these devices are shown in Fig. 23. It can be observed that the PL spectra for low reflectivity thin bottom mirror (Fig. 23 a and b, Fig. 13 a) exhibit very similar behavior regardless of the material used for the mirror. There is some difference in the position of near-infrared cavity mode, which is mainly due to different phase change upon reflection for different materials.[58] For thicker Cu mirror, near-infrared mode becomes more pronounced, but due to lower reflectivity of Cu compared to Ag, behavior with the viewing angle for thick Cu mirror still has more similarity with thin u rather than thick Ag mirror. Based on the obtained results, it can be concluded that the unusual behavior of thick (~200 nm) microcavity devices with low reflectivity bottom mirror is a general feature regardless of the bottom mirror material. Therefore, it should be possible to design microcavity OLEDs with lower reflectivity bottom mirror which do not exhibit blue shift of the emission peak characteristic for thinner devices with highly reflective mirrors. Furthermore, it should be noted that for majority of organic materials having a broad emission spectrum, lower bottom mirror reflectivity is necessary in order to achieve brightness enhancement.[58,59] Thus, low bottom mirror reflectivity represents a realistic design for organic microcavity devices. However, further work is needed in order to fully explain the observed phenomena and conclusively prove or disprove possible polariton emission in thick Alq

based microcavities. Also, from the practical applications points of view, microcavities employing doped organic layers should be considered in order to avoid increase of the driving voltage due to increased organic layer thickness.

4. CONCLUSIONS

We have performed a comprehensive investigation of the organic microcavity light emitting diodes with different organic layer thickness, different emission region position, and different bottom mirror. It was found that the devices with low reflectance bottom mirrors exhibit some unusual features, such as lack of the characteristic blue shift of the emission peak with the viewing angle, significant differences between the EL and PL spectra, as well as differences between PL spectra excited at different wavelengths, which cannot be entirely attributed to the lack of contribution from the NPB layer since the dependence of PL spectra on excitation wavelength was also observed in microcavities containing Alq only. Furthermore, the emitted spectra are strongly dependent on the position of the emission region in the device. This is not the case for the devices with a highly reflective Ag mirror. Plotting the peak positions as a function of the viewing angle resulted in clear anticrossing for the devices with thin Cu mirrors. However, further time-resolved experiments are needed to conclusively establish whether observed phenomena can be attributed to the polariton emission.

ACKNOWLEDGEMENTS

This work is supported by The Research Grants Council of the Hong Kong Special Administrative Region (Project No. HKU 7056/02E and HKBU 2051/02P). The authors would like to thank Dr. J. Gao for the use of step profiler to verify the device thickness.

REFERENCES

[1] A. Dodabalapur, L. J. Rothberg, R. H. Jordan, T. M. Miller, R. E. Slusher, and J. M. Phillips, J. Appl. Phys. **80,** 6954 (1996).

[2] S. Dirr, S. Wiese, H.-H. Johanns, D. Ammermann, A. Böhler, W. Grahn, and W. Kowalsky, Synth. Met. **91**, 53 (1997).

[3] R. H. Jordan, L. J. Rothberg, A. Dodabalapur, and R. E. Slusher, Appl. Phys. Lett. **69**, 1997 (1996).

[4] T. Shiga, H. Fujikawa, and Y. Taga, J. Appl. Phys. **93**, 19 (2003).

[5] N. Tessler, S. Burns, H. Becker, and R. H. Friend, Appl. Phys. Lett. **70**, 556 (1997).

[6] N. Takada, T. Kamata, and D. D. C. Bradley, Appl. Phys. Lett. **82**, 1812 (2003).

[7] P. A. Hobson, W. L. Barnes, D. G. Lidzey, G. A. Gehring, D. M. Whittaker, M. S. Skolnick, and S. Walker, Appl. Phys. Lett. **81**, 3519 (2002).

[8] R. F. Oulton, N. Takada, J. Koe, P. N. Stavrinou, and D. D. C. Bradley, Semicond. Sci. Technol. **18**, S419 (2003).

[9] L. G. Conolly, D. G. Lidzey, R. Butté, A. M. Adawi, D. M. Whittaker, M. S. Skolnick, and R. Airey, Appl. Phys. Lett. **83**, 5377 (2003).

[10] D. G. Lidzey, A. M. Fox, M. D. Rahn, M. S. Skolnick, V. M. Agranovich, and S. Walker, Phys. Rev. B **65**, 195312 (2002).

[11] D. G. Lidzey, D. D. C. Bradley, M. S. Skolnick, T. Virgili, S. Walker, and D. M. Whittaker, Nature **395**, 53 (1998).

[12] D. G. Lidzey, D. D. C. Bradley, M. S. Skolnick, and S. Walker, Synth. Met. **124**, 37 (2001).

[13] D. G. Lidzey, D. D. C. Bradley, A. Armitage, S. Walker, and M. S. Skolnick, Science **288**, 1620 (2000).

[14] P. Schouwink, H. v. Berlepsch, L. Dähne, and R. Mahrt, Chem. Phys. **285**, 113 (2002).

[15] C. Weisbuch, M. Nishioka, A. Ishikawa, and Y. Arakawa, Phys. Rev. Lett. **69**, 3314 (1992).

[16] G. Khitrova, H. M. Gibbs, F. Jahnke, M. Kira, and S. W. Koch, Review of Modern Physics **71**, 1591 (1999).

[17] V. Savona, L. C. Andreani, P. Schwendimann, A. Quattropani, Solid State Commun. **93**, 733 (1995).

[18] C. Y. Hu, H. Z. Zheng, J. D. Zhang, H. Zhang, F. H. Yang, and Y. P. Zeng, Appl. Phys. Lett. **82**, 665 (2003).

[19] K. M. Gustin, Appl. Opt. **26**, 3796 (1987).

[20] G. E. Jellison and B. C. Sales, Appl. Opt. **30**, 4310 (1991).

[21] A. B. Djurišić, C. Y. Kwong, W. L. Guo, T. W. Lau, E. H. Li, Z. T. Liu, H. S. Kwok, L. S. M. Lam, and W. K. Chan, Thin Solid Films **416**, 233 (2002).

[22] M. Brinkmann, F. Biscarini, C. Taliani, I Aiello, and M. Ghedini, Phys. Rev. B **61**, R16339 (2001).

[23] A. D. Rakić, A. B. Djurišić, J. M. Elazar, and M. L. Majewski, Appl. Opt. **37**, 5271 (1998).

[24] R. F. Potter, in *Handbook of Optical Constants of Solids I*, edited by E. D. Palik (Academic Press Inc., San Diego, 1985) p. 11.

[25] E. D. Palik, in *Handbook of Optical Constants of Solids II*, edited by E. D. Palik (Academic Press Inc., San Diego, 1991) p. 8.

[26] H. A. MacLeod, *Thin Film Optical Filters* (Adam Hilger, Bristol, 1986).

[27] B. Harbecke, Appl. Phys. B **39**, 165 (1986).

[28] L. Vriens and M. Rippens, Appl. Opt. **22**, 4105 (1983).

[29] A. H. M. Holtslag and P. M. L. O. Scholte, Appl. Opt. **28**, 5095 (1989).

[30] H. R. Philipp, in *Handbook of Optical Constants of Solids I*, edited by E. D. Palik (Academic Press Inc., San Diego, 1985) p. 749.

[31] A. B. Djurišić and A. D. Rakić, Opt. Commun. **236**, 303 (2004).

[32] A. Dodabalapur, L. J. Rothberg, and T. M. Miller, Appl. Phys. Lett. **65**, 2308 (1994).

[33] X. Liu, D. Poitras, Y. Tao, and C. Py, J. Vac. Sci. Technol. A **22**, 764 (2004).

[34] A. Niko, C. Hochfilzer, T. Jost, W. Graupner, and G. Leising, in: J. r. Raynolds, A. K.-Y. Jen. L. R. Dalton, M. F. Rubner, L. Y. Chiang (Eds.), MRS Fall Meeting 1997, Mat. Res. Soc. Symp. Proc. **488**, 713 (1998).

[35] D. Z. Garbuzov, S. R. Forrest, A. G. Tsekoun, P. E. Burrows, V. Bulovic, and M. E. Thompson, J. Appl. Phys. **80**, 4644 (1996).

[36] F. G. Celii, T. B. Harton, and O. F. Philips, J. Electron Mater. **26**, 366 (1997).

[37] B. Masenelli, S. Callard, A. Gagnaire, and J. Joseph, Thin Solid Films **364**, 264 (2000).

[38] D. W. Lynch and W. R. Hunter, in *Handbook of Optical Constants of Solids I*, edited by E. D. Palik (Academic Press Inc., San Diego, 1985) p. 275.

[39] D. Y. Smith, E. Shiles, and M. Inokuti, in *Handbook of Optical Constants of Solids I*, edited by E. D. Palik (Academic Press Inc., San Diego, 1985) p. 369.

[40] M. Tzolov, W. Brütting, V. Petrova-Koch, A. Mückl, S. Berleb, J. Gmeiner, M. Schwörer, Synth. Met. 119 (2001) 559.

[41] A. Aziz, K. L. Narasimhan, Synth. Met. 131 (2002) 71.

[42] R. J. Curry and W. P. Gillin, J. Appl. Phys. **88**, 781 (2000).

[43] W. Humbs, H. Zhang, and M. Glasbeek, Chem. Phys. **254**, 319 (2000).

[44] R. L. Martin, J. D. Kress, I. H. Campbell, D. L. Smith, Phys. Rev. B **61**, 15804 (2000).

[45] V. V. N. Ravi Kishore, A. Aziz, K. L. Narasimhan, N. Periasamy, P. S. Meenakshi, S. Wategaonkar, Synth. Met. 126 (2002) 199.

[46] V. V. N. Ravi Kishore, K. L. Narasimhan, N. Periasamy, Phys. Chem. Chem. Phys. 5 (2003) 1386.

[47] I. Sokolik, R. Priestley, A. D. Wassler, R. Dorsinville, C. W. Tang, Appl. Phys. Lett. 69 (1996) 4168.

[48] C. W. Tang, S. A. Van Slyke, C. H. Chen, J. Appl. Phys. 85 (1989) 3610.

[49] S. K. So, W. K. Choi, L. M. Leung, and K. Neyts, Appl. Phys. Lett. **74**, 1939 (1999).

[50] S. Naka, H. Okada, H. Onnagawa, Y. Yamaguchi, and T. Tsutsui, Synth. Met. **111-112**, 331 (2000).

[51] W. Brütting, H. Riel, T. Beierlein, and W. Reiss, J. Appl. Phys. **89**, 1704 (2001).

[52] S. Berleb, W. Brütting, and G. Paasch, Synth. Met. **122**, 37 (2001).

[53] M. Matsumura, A. Ito, and Y. Miyamae, Appl. Phys. Lett. **75**, 1042 (1999).

[54] D. Y. Kondyakov, J. R. Sandifer, C. W. Tang, and R. H. Young, J. Appl. Phys. **93**, 1108 (2003).

[55] B. Ruhstaller, S. A. Carter, S. Barth, H. Riel, W. Riess, and J. C. Scott, J. Appl. Phys. **89**, 4575 (2001).

[56] M. Matsumura and Y. Jinde, Synth. Met. **91**, 197 (1997).

[57] M. Matsumura and Y. Jinde, IEEE Trans. Electron Dev. **44**, 1229 (1997).

[58] A. B. Djurišić and A.D.Rakić, Appl. Opt. **41**, 7650 (2002).

[59] H. Benisty, H. De Neve, and C. Weisbuch, IEEE Journal of Quantum Electronics **34**, 1612 (1998).

TABLES

Table I Lorentz and Lorentz-Drude model parameters obtained by fitting the spectroscopic ellipsometry data for Alq, NPB, Ag, and Cu.

parameters	Alq	NPB	Ag	Cu
ε_{inf}	1.96	1.82	4.45	1.00
F_0 (eV^2)	---	---	86.7	54.27
Γ_0 (eV)	---	---	0.03	0.21
ω_1 (eV)	3.17	3.57	4.22	2.53
F_1 (eV^2)	0.83	3.42	5.78	3.80
Γ_1 (eV)	0.58	0.59	0.27	0.58
ω_2 (eV)	3.82	5.16	---	3.83
F_2 (eV^2)	0.25	16.05	---	42.18
Γ_2 (eV)	0.47	0.41	---	2.80
ω_3 (eV)	5.10	---	---	9.00
F_3 (eV^2)	17.08	---	---	192.62
Γ_3 (eV)	0.28	---	---	6.00

FIGURE CAPTIONS

Fig. 1 Experimental and calculated TanΨ and CosΔ of Alq film on Si substrate for three different incident angles.

Fig. 2 Experimental and calculated TanΨ and CosΔ of NPB film on Si substrate for three different incident angles.

Fig. 3 The real and imaginary parts of the refractive index of Alq and NPB.

Fig. 4 Experimental and calculated TanΨ and CosΔ of Cu film on a glass substrate for three different incident angles.

Fig. 5 Experimental and calculated TanΨ and CosΔ of Cu film on a glass substrate for three different incident angles.

Fig. 6 The real and imaginary parts of the refractive index of Ag and Cu.

Fig. 7 Electroluminescence spectra of the Cu (25 nm)/NPB (65 nm)/Alq (139 nm)/Ag (70 nm) device for different incident angles.

Fig. 8 Photoluminescence spectra of the Cu (25 nm)/NPB (65 nm)/Alq (139 nm)/Ag (70 nm) device for different incident angles from a) Cu side b) Ag side. Excitation wavelength was 325 nm.

Fig. 9 Photoluminescence spectra for different incident angles of the devices with NPB/Alq thickness a) 33/69 and b) 130/278. Excitation wavelength was 325 nm.

Fig. 10 Electroluminescence (a) and photoluminescence spectra through bottom Ag (b) and top Ag (c) mirror of the 33/69 device for different incident angles. Excitation wavelength was 325 nm.

Fig. 11 Electroluminescence spectra for different incident angles for different position of the NPB/Alq interface a) 153/51; b) 102/102; c) 51/153; d) 26/178.

Fig. 12 Photoluminescence spectra for different incident angles for different position of the NPB/Alq interface a) 153/51; b) 102/102; c) 51/153; d) 26/178. Excitation wavelength was 325 nm.

Fig. 13 Photoluminescence spectra of the devices with 204 nm Alq for a) Cu (25 nm) bottom mirror b) Ag (80 nm) bottom mirror. Excitation wavelength was 325 nm.

Fig. 14 Photoluminescence spectra from the top Ag electrode for the devices a) 153/51, Cu mirror b) 51/153, Cu mirror, c) 153/51, Ag mirror d) 51/153, Ag mirror. Excitation wavelength 325 nm.

Fig. 15 Comparison between the calculated and measured EL spectra for different NPB/Alq interface position a) Cu 25 nm bottom mirror b) Ag 80 nm bottom mirror. All the spectra correspond to 0° viewing angle.

Fig. 16 Influence of the thickness of the emitting region on the calculated spectra for 51/153 device for a) Cu bottom mirror (25 nm) b) Ag bottom mirror (80 nm).

Fig. 17 Photoluminescence of a) 33/69, b) 65/139, and c) 130/278 devices. Excitation wavelength is 420 nm.

Fig. 18 Photoluminescence of microcavity with 204 nm Alq. Excitation wavelengths are a) 420 nm and b) 488 nm.

Fig. 19 Reflectance (experimental (a) and calculated (b)) and transmittance (experimental (c) and calculated (d)) spectra for different incident angles for device with organic layer thickness 51/153 and 25 nm Cu mirror.

Fig. 20 Reflectance spectra of 204 nm Alq microcavity with (a) 25 nm Cu bottom mirror (b) 80 nm Ag mirror.

Fig. 21 Dispersion curves for the device with 204 nm Alq layer for a) 80 nm Ag mirror b) 25 nm Cu mirror. Fit of the transmission peaks of the device with Cu mirror to the three coupled oscillator model[12,13] is also shown. Obtained parameters are: refractive index n=1.5, Interaction potentials V_1=0.42 and V_2=0.45, photon energy $E_{ph}(0)$=1.839 eV, and exciton energies E_{ex1}=2.314 eV and E_{ex2}=2.038 eV.

Fig. 22 Dispersion curves for the 51/153 device with a) 80 nm Ag mirror b) 25 nm Cu mirror. Fit of the transmission peaks of the device with Cu mirror to the two coupled oscillator model[8] is also shown. Obtained parameters are: refractive index n=1.67, interaction potential $V=E_R/2$=0.12, photon energy $E_{ph}(0)$=2.275 eV, and exciton energy E_{ex}=2.428 eV.

Fig. 23 Photoluminescence of 204 nm Alq microcavities with a) 17 nm thick Ag mirror b) 28 nm thick Au mirror and c) 60 nm thick Cu mirror.

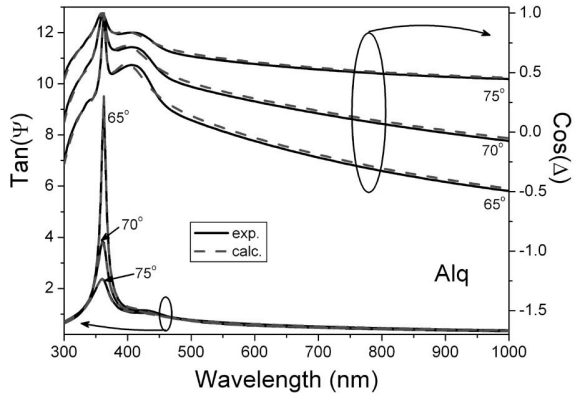

Fig. 1

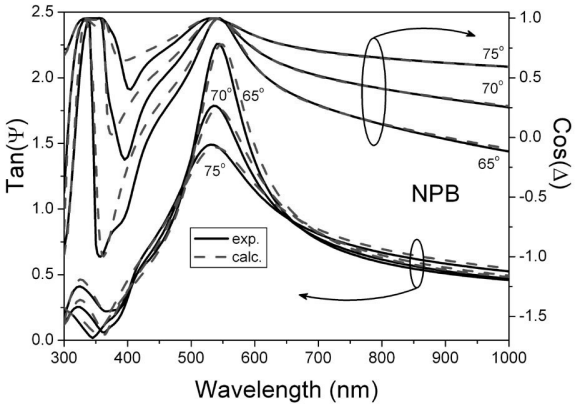

Fig. 2

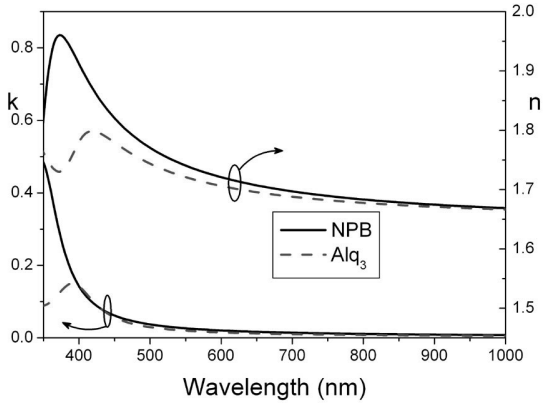

Fig. 3

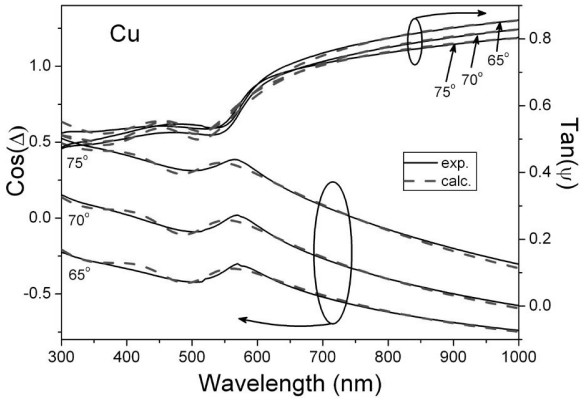

Fig. 4

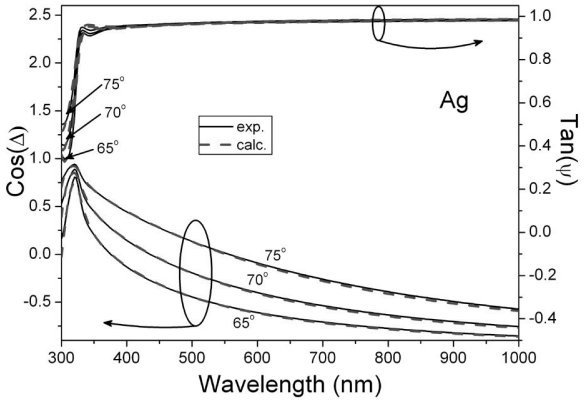

Fig. 5

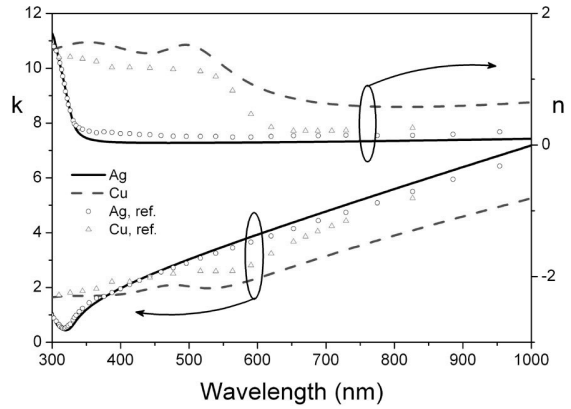

Fig. 6

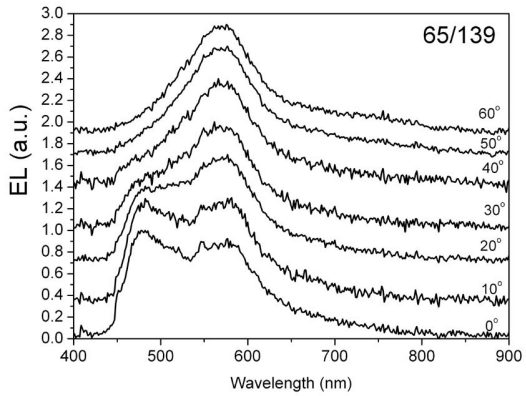

Fig. 7

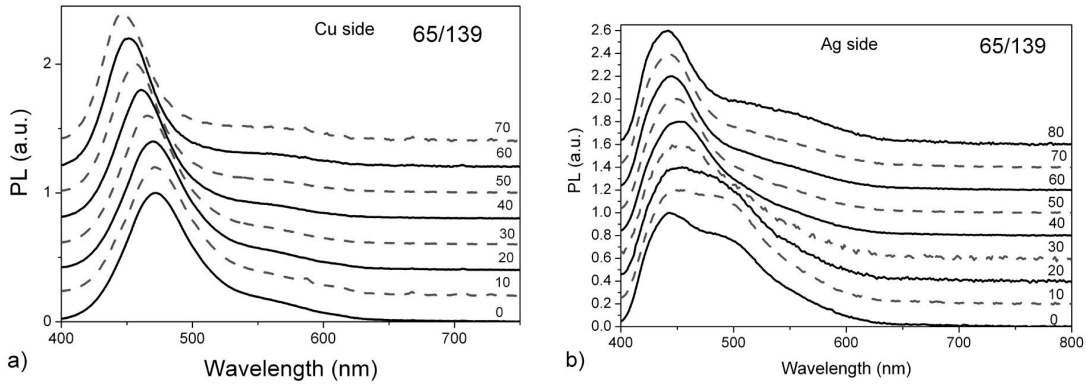

Fig. 8

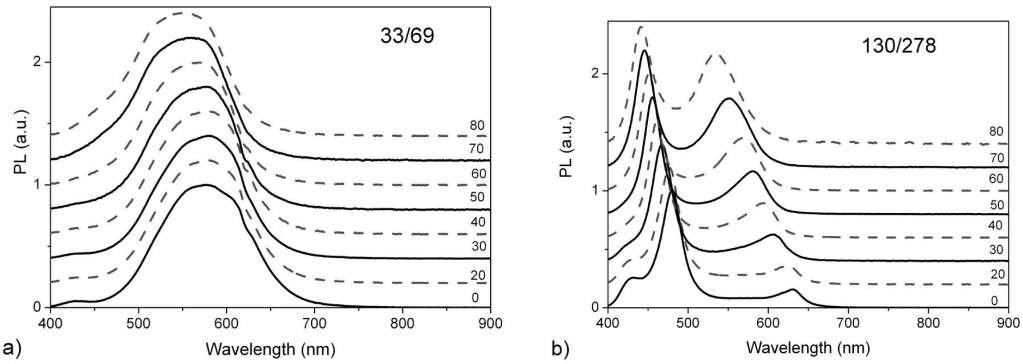

Fig. 9

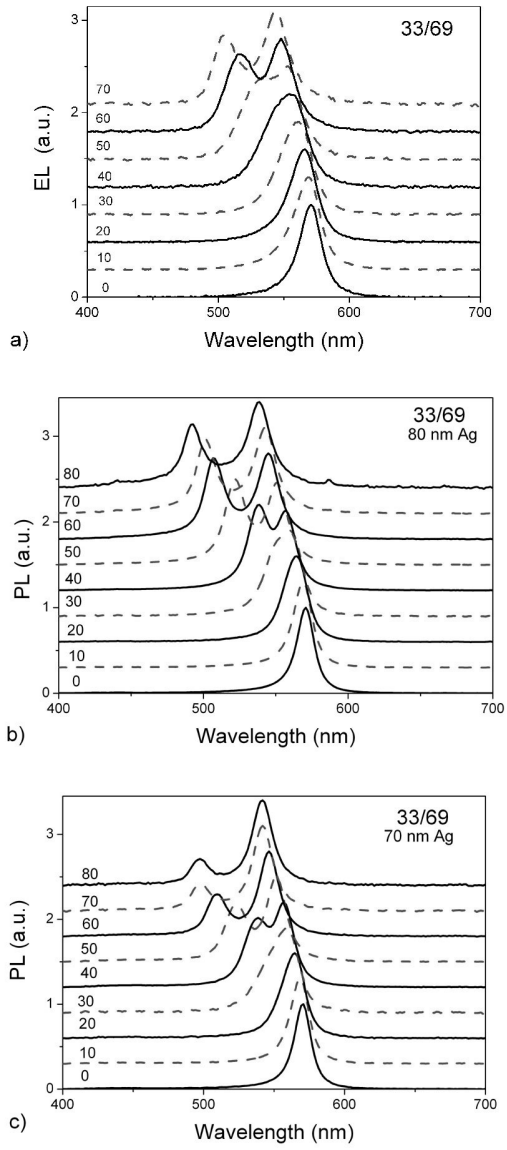
33/69
EL (a.u.)
Wavelength (nm)
a)
33/69
80 nm Ag
PL (a.u.)
Wavelength (nm)
b)
33/69
70 nm Ag
PL (a.u.)
Wavelength (nm)
c)

Fig. 10

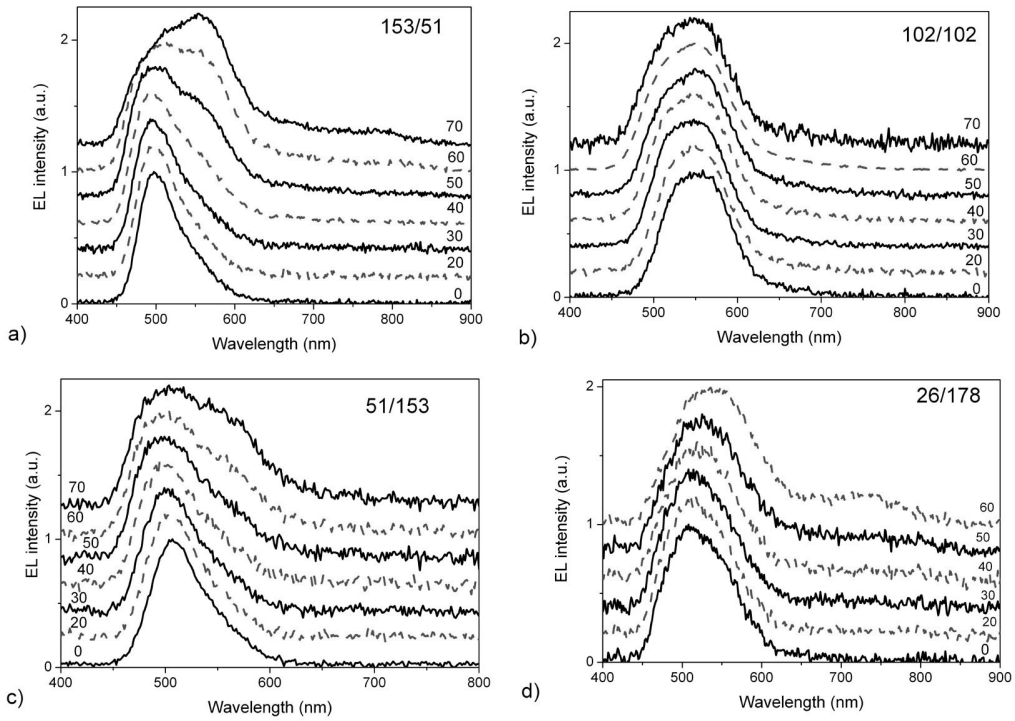
153/51
102/102
51/153
26/178
EL intensity (a.u.)
Wavelength (nm)
a)
b)
c)
d)

Fig. 11

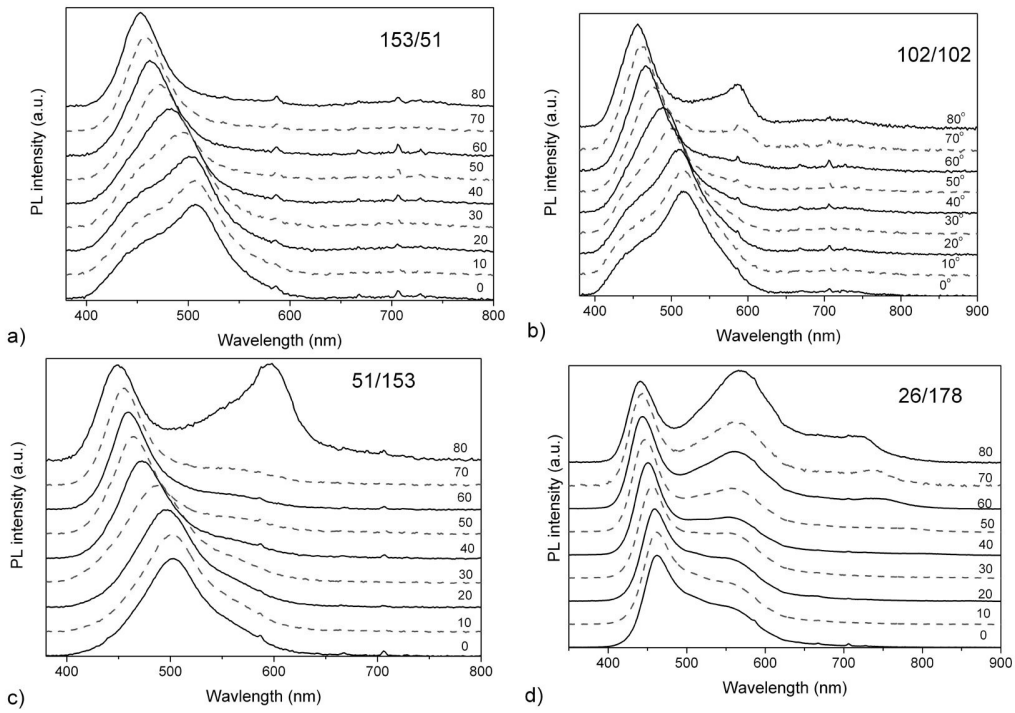
153/51
102/102
51/153
26/178
PL intensity (a.u.)
Wavelength (nm)
Wavlength (nm)
a)
b)
c)
d)

Fig. 12

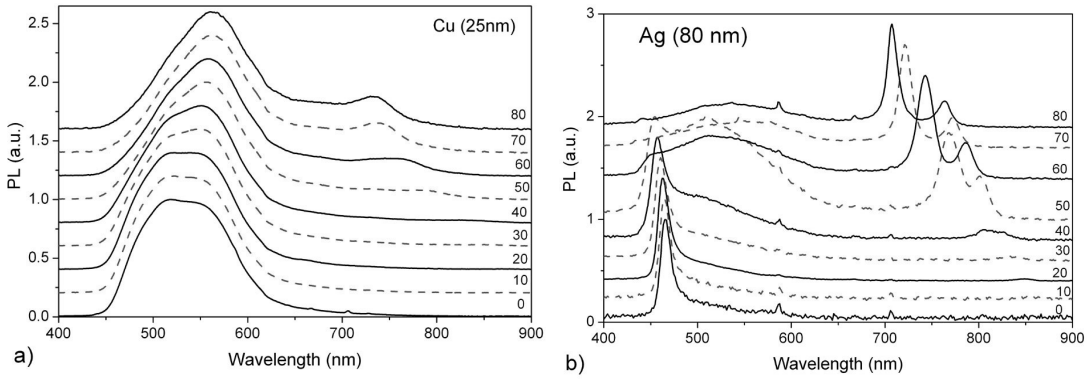
Cu (25nm)
PL (a.u.)
Wavelength (nm)
a)
Ag (80 nm)
PL (a.u.)
Wavelength (nm)
b)

Fig. 13

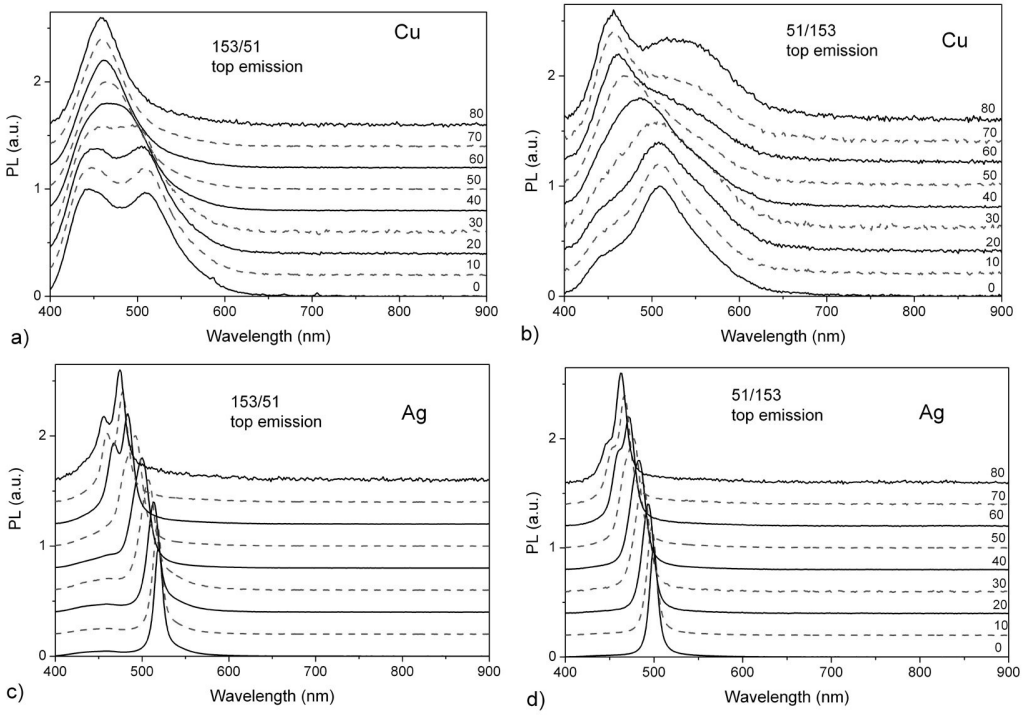
153/51
top emission
Cu
PL (a.u.)
Wavelength (nm)
a)
51/153
top emission
Cu
PL (a.u.)
Wavelength (nm)
b)
153/51
top emission
Ag
PL (a.u.)
Wavelength (nm)
c)
51/153
top emission
Ag
PL (a.u.)
Wavelength (nm)
d)

Fig. 14

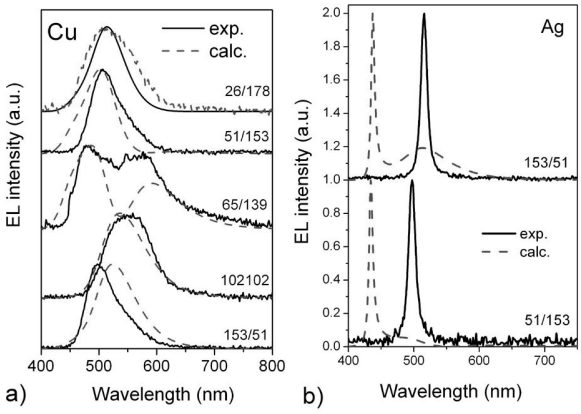
Cu
exp.
calc.
26/178
51/153
65/139
102102
153/51
EL intensity (a.u.)
Wavelength (nm)
a)
Ag
153/51
exp.
calc.
51/153
EL intensity (a.u.)
Wavelength (nm)
b)

Fig. 15

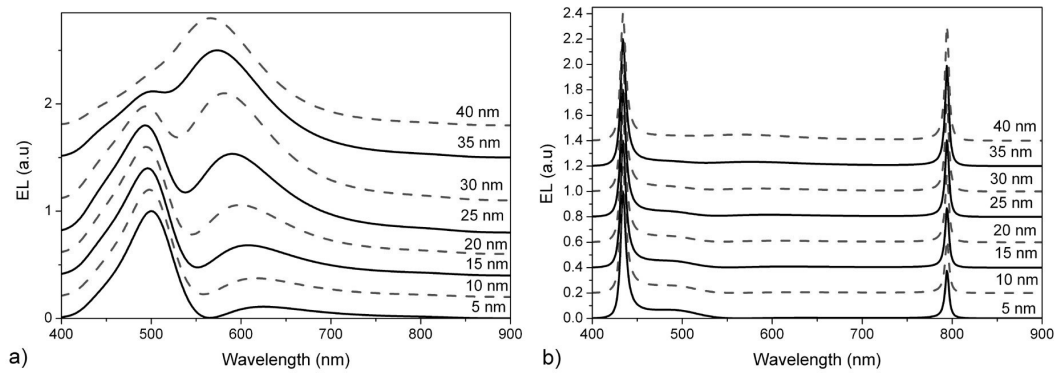
40 nm
35 nm
30 nm
25 nm
20 nm
15 nm
10 nm
5 nm
EL (a.u)
Wavelength (nm)
a)
b)

Fig. 16

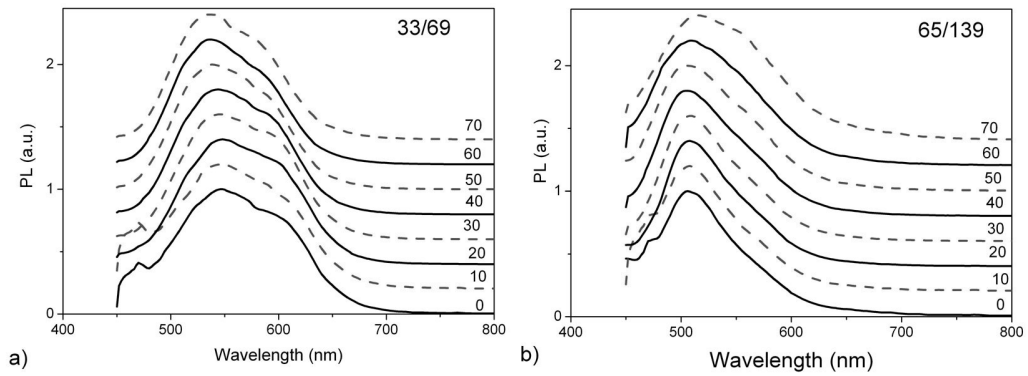
33/69
65/139
70
60
50
40
30
20
10
0
PL (a.u.)
Wavelength (nm)
a)
b)

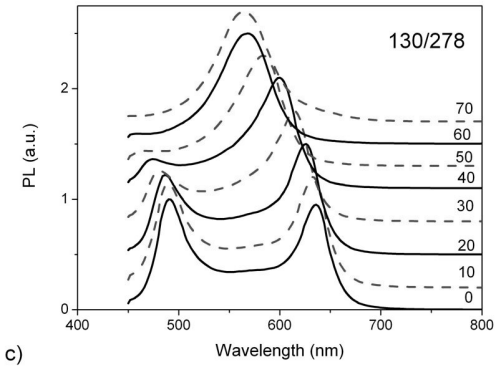
130/278
PL (a.u.)
Wavelength (nm)
70
60
50
40
30
20
10
0
c)

Fig. 17

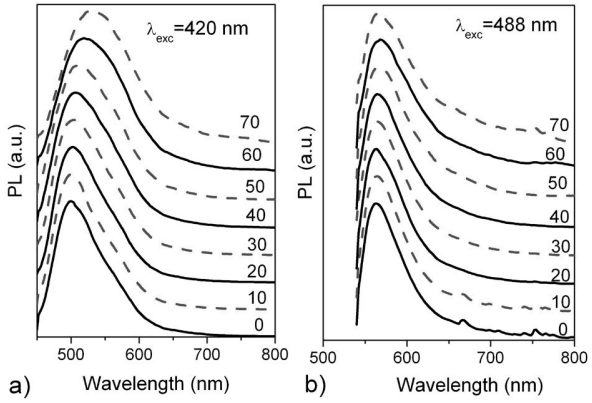
λexc=420 nm
λexc=488 nm
PL (a.u.)
Wavelength (nm)
70
60
50
40
30
20
10
0
a)
b)

Fig. 18

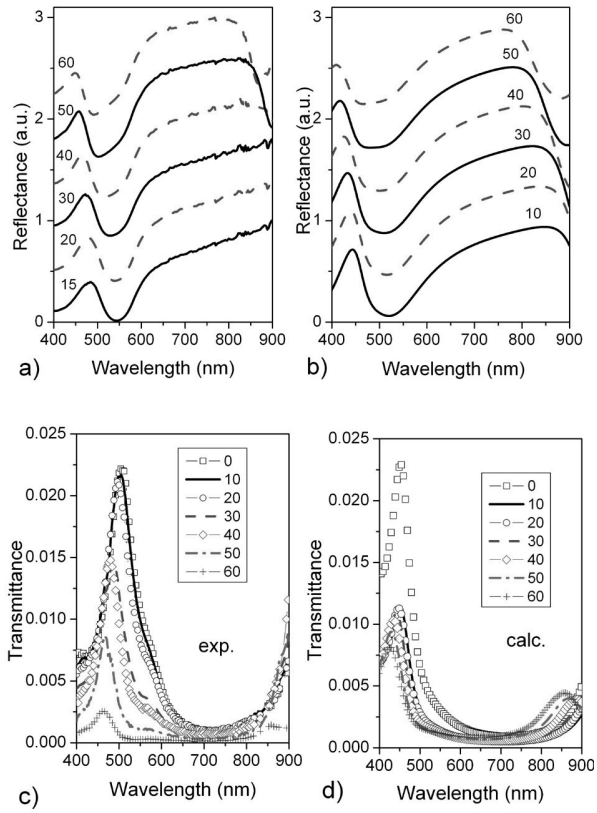
Reflectance (a.u.)
Wavelength (nm)
a)
b)
60
50
40
30
20
15
10
Transmittance
exp.
calc.
c)
d)
0
10
20
30
40
50
60

Fig. 19

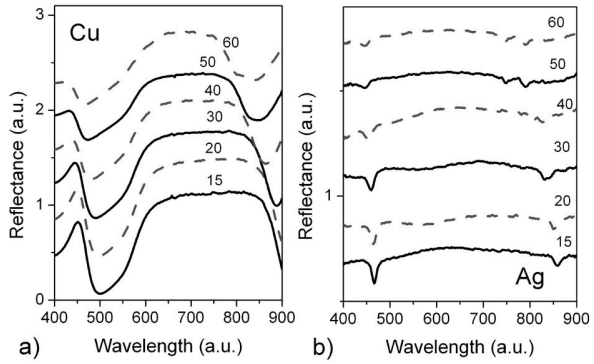
Cu
Ag
Reflectance (a.u.)
Wavelength (a.u.)
a)
b)
60
50
40
30
20
15

Fig. 20

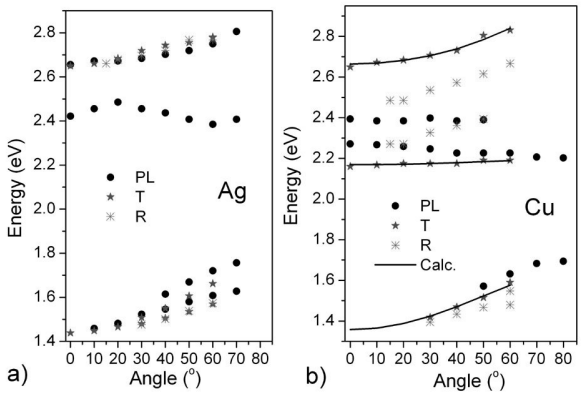
Energy (eV)
Angle (°)
PL
T
R
Ag
a)
Calc.
Cu
b)

Fig. 21

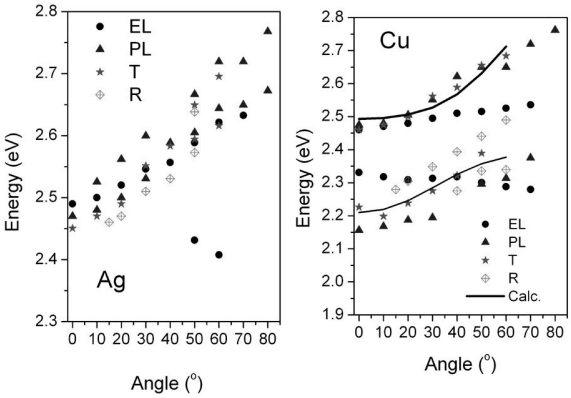
EL
PL
T
R
Ag
Cu
Calc.
Energy (eV)
Angle (°)

Fig. 22

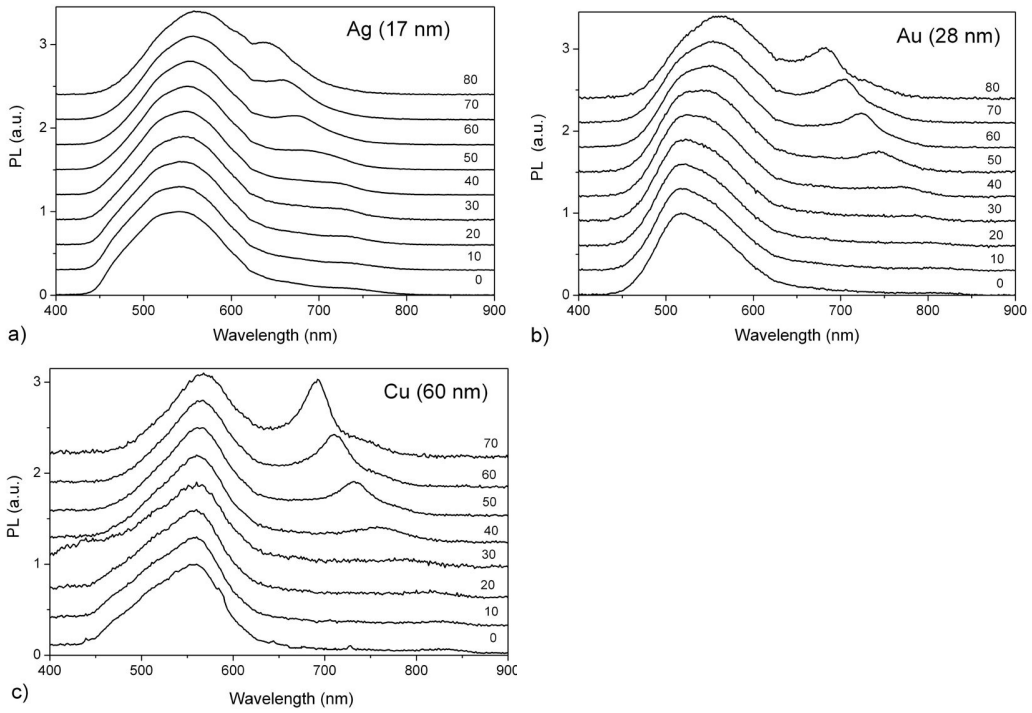

Fig. 23